# BLACK SHALE DEPOSITION AND EARLY DIAGENETIC DOLOMITE CEMENTATION DURING OCEANIC ANOXIC EVENT 1: THE MID-CRETACEOUS MARACAIBO PLATFORM, NORTHWESTERN SOUTH AMERICA

DANIEL A. PETRASH, NUR GUENELI, JOCHEN J. BROCKS, JOSE A. MÉNDEZ, GABRIELA GONZALEZ-ARISMENDI, SIMON W. POULTON, and KURT O. KONHAUSER

#### SUPPLEMENTARY INFORMATION

#### FURTHER GEOLOGICAL BACKGROUND

In terms of sequence stratigraphy, three out of six mixed carbonate/clastic 'glacio-eustatic: sequences that have been recognized within the Cogollo Group (for example Vahrenkamp and others, 1993) are within the Apón Formation; with three others pertaining to the overlying Lisure and Maraca formations. During relative sea level rises, the shallow marine environments were sites for the deposition of grainstone/rudstone interbar deposits. By contrast, the high sea level progradational cycles produced extended low-energy restricted shallow-marine environments, represented by lagoonal sediments rich in organic matter (Bartok and others, 1981; Vahrenkamp and others, 1993). Within these facies, miliolid-rich foraminiferal wackestones and dolomitic shales represent restricted lagoonal and tidal flat settings (Bartok and others, 1981). An alternative view is that the carbonate ramp may also have been episodically affected by drowning, such that, in previously shallow-water areas, black shales rest on condensed basal transgressive lags or unconformities, which in turn, rest on shallow-water facies (Perez-Infante, 1996).

Although the lithofacies comprising the Apón Formation are generally thought to represent sedimentation in a humid climate zone (Vahrenkamp and others, 1993), by the time of deposition of the Guáimaros Member, the ramp would have been affected by a more complex and dynamic climatic regime:

i) When present, the impoverished faunal assemblage of the Guáimaros Shale consists of small-sized individuals (see Ford and Houbolt, 1963), suggestive of conditions not suitable for the colonization of stenohaline species.

- ii) The presence of *Weichselia* sp. plant fragments (Renz, 1982, and references therein) a xerophytic fossil of a fern like angiosperm common in Aptian to Albian sedimentary successions of South America (Edwards, 1933). This is often interpreted as inhabiting coastal mudflats (for example Smith and others, 2001; Schweitzer and others, 2003), but would rather be representative of semi arid climate regimes (see Sender and others, 2005 for details). *Weichselia* sp. would therefore, be a record of heterogeneities in the paleolittoral system that resulted in the colonization of the coastal zone by mangrove-like vegetation (Lacovara and others, 2000, 2003).
- iii) The cryptomicrobial primary sedimentary features of Guáimaros lithology *sensu stricto* and the Guáimaros like microfacies, includes crinkled laminar textures and is rarely bioturbated (Bartok and others, 1981), which suggests that its organic content (>1.1, up to 5.0 wt. % TOC) would have partially resulted from the cyclic burial of microbial mats (for example Mazzullo and Friedman, 1977).

# REFERENCES FOR FURTHER GEOLOGICAL BACKGROUND

- Alberdi-Genolet, M. and Tocco, R., 1999, Trace metals and organic geochemistry of the Machiques Member (Aptian–Albian) and La Luna Formation (Cenomanian–Campanian), Venezuela: Chemical Geology, v. 160, p. 19–38.
- Bartok, P., Reijers, T., and Juhasz, I., 1981, Lower Cretaceous Cogollo Group, Maracaibo Basin, Venezuela: sedimentology, diagenesis, and petrophysics: American Association of Petroleum Geologists Bulletin, v. 65, p. 1110–1134
- Edwards, W., 1933, On the Cretaceous fern *Paradoxopteris* and its connexion with *Weichselia*: Annals of Botany, v. 2, p. 317–341.
- Ford, A.B., Houbolt, J.J.H.C., 1963, The microfacies of the cretaceous of western Venezuela. EJ Brill., 55 p.
- Lacovara, K. J., Smith, J. R., Smith, J.B., Lamanna, M.C., and Dodson. P., 2000, Paralic environments of the Cretaceous dinosaurs of Egypt: a discussion of uniformitarian analogs: Journal of Vertebrate Paleontology, v. 20. p. 53.
- Lacovara, K. J., Smith, J. R., Smith, J. B., and Lamanna, M. C., 2003, The Ten Thousand Islands Coast of Florida: A modern analog to low-energy mangrove coasts of Cretaceous epeiric seas, *in* Davies, R.A.J., editor, Proceedings of the 5th International Conference on Coastal Sediments, Clearwater Beach, Florida: CD-ROM Published by World Scientific Publishing Corporation and East Meets West Productions, Corpus Christi, Texas, p. 1773–1784.
- Mazzullo, S., Friedman, G., 1977, Competitive algal colonization of peritidal flats in a schizohaline environment: The Lower Ordovician of New York: Journal of Sedimentary Research, v. 47, p. 398–410.

- Perez-Infante, J., 1996, Global and local controls upon the deposition of organic-rich Cretaceous sequences of Western Venezuela: a geochemical study: Ph.D. thesis, University of Newcastle, Tyne, UK.
- Renz, O., 1982, The Cretaceous ammonites of Venezuela: Basel, Birkhauser Verlag, 132 p. (+ 40 plates).
- Schweitzer, C.E., Lacovara, K.J., Smith, J.B., Lamanna, M.C., Lyon, M.A., Attia, Y., , 2003, Mangrove dwelling crabs (Decapoda: Brachyura: Necrocarcinidae) associated with dinosaurs from the upper Cretaceous (Cenomanian) of Egypt: Journal of Paleontology, v. 77, p. 888–894.
- Smith, J.B., Lamanna, M.C., Lacovara, K.J., Dodson, P., Smith, J.R., Poole, J.C., Giegengack, R., and Attia, Y., 2001, A giant sauropod dinosaur from an Upper Cretaceous mangrove deposit in Egypt: Science, v. 292, p. 1704 1706.

#### **DETAILED METHODS**

# Mineralogical and Textural Features

The mineralogical and textural features were analyzed via standard petrography, and Scanning Electron Microscopy (SEM) coupled to Electron Dispersive Spectrometry (EDS). Other analyses included X ray Diffraction (XRD) to evaluate the mineralogy of the clay fraction, and Electron Probe Microanalyses to assess minor variations in the Mg:Ca ratio of dolomite crystals.

SEM-EDS.— SEM observations were performed on a JEOL JSM-6301FXV that has an attached Norvar energy dispersive spectrometer system (PGT). Most photomicrographs were taken at 5 kV, but some involving complementary EDS were conducted at 20 kV. A constant working distance of 15 mm was used throughout our SEM-EDS analyses. Some samples were treated with 10 s immersion in 10% HCl, in order to reveal microtextural features resulting from the preferential dissolution of high Ca – dolomite (> 55 mol % CaCO<sub>3</sub>; Jones and others, 2001).

Clay mineralogy.— The <0.2 μm fraction of the clays were characterized via XRD by Bernabe Aguado at the Venezuelan Institute of Petroleum Technology (INTEVEP). Chemical pre-treatments performed prior to analysis included acetate buffer reaction to remove the carbonate fraction; organic matter removal via H<sub>2</sub>O<sub>2</sub> reaction at 80°C; immersion into a sodium chloride, acetone, and methanol solution, to remove the amorphous organic fraction; and removal of iron oxides via dithionite. Oriented preparations were made by centrifugation followed by pressing the dried preparation upside down against absorbent paper, with one subsample previously wetted with ethylene glycol. The composites remained overnight in this

position. XRD patterns were recorded from 2 to 35 (20) degrees using Ni-filtered Cu\_K $\alpha$  radiation. Slits were selected so that the X ray beam divergence was less than the sample length. The patterns were collected automatically by step-scanning at 0.02° (20) intervals using a 1 s counting time per step. Quantitative analyses of the samples were determined by comparing the air – dried and glycol – solvated patterns (Moore and Reynolds, 1989).

*EPMA*.— The major element distribution of the dolomite crystals comprising three representative samples was determined using Wavelength Dispersive Spectroscopy (WDS) in a JEOL JXA-8900 instrument operated at 15 kV accelerating voltage, focused beam diameter and an average current of 10 nA. WDS analyses were achieved by setting count times of 20 s on each peak and half the peak count time on each background. Detection limits (3σ) from the average of three analyses are ~250 ppm for both MgO and CaO oxides. A combination of natural minerals was used to reduce counts to weight percent concentrations using the CITZAF method, with matrix corrections as implemented by P. Carpenter (Caltech, 1993). The mineral crystals used as primary standards were Eugi (Spain) dolomite (MgO), and Big Horn (MO, USA) calcite (CaO).

#### **Biomarkers**

*Microablation.*— Samples were processed according to the micro – ablation technique described by Jarrett and others (2013). Laboratory blanks contained near-zero background levels, signifying that hydrocarbons detected in the samples are not cross contamination or instrumental contamination during experimental procedures.

Extraction and fractionation of extractable organic matter.— Bitumen was extracted from 3 – 8 g of rock powder using an Automated Solvent Extractor (ASE 200, Dionex) with dichloromethane and methanol (9:1 v/ v) as solvents. Instrumental settings were as following: preheat 2 min, heat 5 min, static 2 min, flush 100%, purge 30 s, 5 cycles, 1000 PSI and 100 °C. The extracts were reduced in volume (< 1 ml) under a stream of purified nitrogen gas and then left to evaporate at room temperature.

Extractable organic matter (1 mg) was placed onto a dry-packed silica (annealed at 250°C/9h, grade 60, 70 – 230 mesh, ThermoFisher Scientific) column (4 mm internal diameter) and was air dried overnight. Extracts were separated by column chromatography into saturated,

aromatic, and polar fractions. Saturated hydrocarbons were eluted with 1.5 dead volumes (DV) *n*-hexane, aromatic hydrocarbons with 2 DV *n*-hexane:dichloromethane (4:1 v/v) and polar compounds with 2.5 DV dichloromethane: methanol (1:1 v/v). Fractions were air-dried. Elemental sulfur was removed from the saturated fractions by filtration over freshly precipitated elemental copper (Brocks and others, 2005).

Gas chromatography – mass spectrometry (GC – MS).— Molecular components of saturated and aromatic hydrocarbon fractions were identified by a GC-MS system, consisting of a Waters AutoSpec Premier double – sector mass spectrometer interfaced with a 6890 GC (Agilent), fitted with a DB – 5MS capillary column (60 m length, 0.25 mm internal diameter, 0.25 µm film thickness (J&W Scientific). Helium was used as the carrier gas at a constant flow of 1 ml/min. Samples were initially injected in split-less mode into a Gerstel PTV injector at a temperature of 60 °C, held for 0.1 min and then heated at 260 °C/min to 300 °C. For any run, the GC oven was programmed at 60 °C (4 min), heated to 315 °C at 4 °C/ min, with a final hold time of 22 to 52 min. The MS source was operated at 260 °C in EI+ mode at 70 eV ionization energy and with 8000 V acceleration voltage. Saturated and aromatic fractions were analysed in full scan mode over a mass range of 55 – 600 Da, with a scan duration of 0.7 s and interscan delay of 0.2 s. Saturated fractions were further analysed by multiple reaction monitoring (MRM) with a total cycle time of  $\sim 1.2$  s for function 1 ( $\sim 1.1$  s cycle time, 0.1 s delay) and  $\sim 1.5$  s for function (~1.4 s cycle time, 0.1 s inter-scan delay) for 42 transitions in total. Aromatic hydrocarbons were further analysed by selected ion recording (SIR) under magnet control with a total cycle time of  $\sim 0.85$  s (0.75 s cycle time, 0.1 s inter – scan delay) for thirteen ions. All samples were injected in hexane to avoid deterioration of chromatographic signals due to the build – up of FeCl<sub>2</sub> in the ion source (see Brocks and Hope, 2014).

*Peak identification and quantification.*— Isoprenoid and aryl isoprenoid derivatives were identified by comparing spectra, elution times and patterns with laboratory reference material (Brocks and Summons, 2003; Brocks and others, 2005).

Statistical Analyses.—A Shapiro-Wilk's test of normality was used to determine whether our environmental parameters follow a normal distribution. The parameters were then scaled for ordination in commensurable units, and analyzed using principal component analysis (PCA), with the correlation matrix that resulted from a Spearman correlation test as input data. PCA or

eigenvector analysis simplifies complex n-dimensional data, where n is the number of variables, by transforming the original variables into a new set of variables. Thus, the objective of the PCA was to reduce the dimensionality of our geochemical data to a few eigenvectors that best explain the variation in the data. The relationships between samples are not changed by this transformation. The parameters were categorized using the first principal component, PC1. All correlation coefficients defining our categories are normally distributed and had a significance level of P < 0.05. Other variables that do not seem to follow a normal distribution, that is their computed p-value is lower than the significance level  $\alpha = 0.05$  in the normality test (for example %C<sub>28</sub>, %C<sub>30</sub>, 28,30BNH, Pr/Ph, Pr/Pr\*, [Mo], Hf and Ta), were also scaled and incorporated in the PCA. The incorporation of such non-normally distributed parameters in the PCA does not produce any significant change in the PC clustering, and the "risk" to consider them normally distributed is lower than 3.8% in all cases, and lower than 0.5% for Pr/Ph and the inorganic parameters.

General notes.— The biomarker analyses were conducted at the Australian National University following rigorous protocols to exclude anthropogenic hydrocarbon contaminants that commonly taint drill core material (Jarrett and others, 2013). Because this study focuses in a specific microfacies, a stratigraphical analysis was not attempted but only the variability and correlation of parameters between samples were assessed in order to determine the environmental control(s) governing their deposition.

#### Major, Minor and Trace Element Analyses

Bulk analyses.— Bulk samples were first ground with an agate mortar and pestle. The homogenized ground powder was used for all subsequent bulk geochemical analyses conducted at the University of Alberta. For major, minor and trace element analyses bulk rock minor and trace elements were determined after digestion with a 4:1 mixture of hydrofluoric and nitric acids. The samples were digested in a platinum crucible with a solution of concentrated HNO<sub>3</sub> (2 mL) and HF (8 mL) to near dryness; subsequently a second addition of concentrated HCl (5 mL) and HNO<sub>3</sub> (5 mL) was made and again the mixture was evaporated to near dryness. The residue was then dissolved in 10 mL of 8 N HNO<sub>3</sub> and diluted to ~20 mL with 8.8 mL ultrapure water, 0.1 mL HNO<sub>3</sub>. A 0.1 mL of a Br, In, and Sc spike was added. Samples were then analyzed on an Perken Elmer Elan6000 Inductively Coupled Plasma Quadrupole Mass Spectrometry (ICPQ-MS)

device, and instrument operating conditions are as follows: RF power = 1200 W; dual detector mode; blank subtraction performed subsequent to internal standard correction; unit of measurement is cps (counts per second); auto lens on; use of 4-point calibration curves (0, 0.25, 0.50, and 1.00 ppm for Ca, Mg, and Fe; 0.005, 0.010, and 0.020 ppm for the remaining elements); sample uptake rate (using a peristaltic pump) was ~1 mL; sample analysis consisted of 35 sweeps/reading, 1 reading/replicate and 3 replicates; dwell times were 10 ms for Al, Mn, and U, and 20 ms for the remaining elements; total integration times (dwell time x number of sweeps) were 350 ms for Al, Mn, and U, and 700 ms for the remaining elements (table 1). External reproducibility, based on repeated analysis of international whole rock standard (Granodiorite, Silver Plume, Colorado, GSP-2) is 5 - 10% ( $2\sigma$  level) for most elements. None of the reported minor element values were corrected for non – lattice bound metal contamination, which would have required pore water measurements (Staudt and others, 1993). However, for some metals a comparison of bulk rock vs. intracrystalline concentrations, elements measured using laser ablation ICPQ-MS (see below), were used for that purpose.

The total organic carbon (TOC) values were determined in carbonate – free samples using a combustion – infrared absorption method at a LECO CS-244 analyzer, and are composed of pyrolyzable carbon and additional CO and CO<sub>2</sub> groups released during oxidation of the residual organic carbon.

The normalization – values to evaluate transition metal concentrations are from Wedepohl, (1978). However, to facilitate comparison of rare earth elements (REE) patterns for different samples, the abundances of the individual REE were divided by the abundances in average post-Archean Shales (PAAS), with "SN" standing for PAAS-normalized concentrations (Nance and Taylor, 1976). We focused mostly on the geochemistry of the redox – sensitive element cerium, and its neighbor elements La and Pr, but the ratio of heavy (HREE) vs. light (LREE) rare earths, Er/Nd, was also evaluated, as it offers a useful criterion to infer early diagenetic chemical changes likely to be caused by differential rates of siliciclastic input.

The Ce anomaly was determined by evaluating the  $Pr/Pr^*$  ratio of unity, where ( $Pr^*=0.5Ce+0.5Nd$ )<sub>SN</sub>. This calculation prevents biases caused by the occurrence of positive La anomalies in seawater – derived precipitates, which may result in an apparent Ce anomaly (for example, de Baar and others, 1991). The significance of the Ce anomaly, as an indicator of

anoxicity, was further assessed by applying an alternative criteria, developed by de Baar and others (1988), which states that only when the expression  $Ce_{anom} = [3Ce/(2La + Nd)]_{SN} > 1.0$  would precipitation have occurred under anoxic conditions. La was studied by using the expression  $Ce/Ce^*$  and the Y/Ho ratio was used to quantify the extent of detrital input to the plasma produced via Laser Ablation Inductively Coupled Plasma Quadrupole Mass Spectrometry (see Kamber and Webb, 2004 for details).

Fe speciation.— Fe speciation analyses were conducted at the University of Leeds. We used well – calibrated iron extraction techniques to explore the shallow marine redox conditions of deposition, where highly reactive iron (Fe<sub>HR</sub>) represents the iron that may be geochemically and biologically active during early sediment diagenesis (Canfield and others, 1992; Poulton and others, 2011). A sequential extraction scheme (Poulton and Canfield, 2005) was implemented to partition iron into its highly reactive components and its unreactive phases. This scheme recognizes a variety of operationally defined iron pools, comprising ferric oxides extracted with dithionite (Fe<sub>ox</sub>), carbonate-associated Fe extracted with acetate (Fe<sub>carb</sub>), and magnetite Fe extracted with oxalate (Fe<sub>mag</sub>). Pyrite Fe (Fe<sub>Py</sub>) was determined separately via chromous chloride distillation (Canfield and others, 1986). Highly reactive Fe was then calculated as Fe<sub>HR</sub> = Fe<sub>Py</sub> + Fe<sub>carb</sub> + Fe<sub>ox</sub> + Fe<sub>mag</sub> (Poulton and others, 2011). The operational defined ratios from iron speciation, Fe<sub>HR</sub> to total Fe (Fe<sub>HR</sub>/Fe<sub>T</sub>; Raiswell and Canfield, 1998) and Fe<sub>Py</sub> to Fe<sub>HR</sub> (Fe<sub>Py</sub>/Fe<sub>HR</sub>) are presented in a cross – plot (after Shen and others, 2002).

Stable carbon and oxygen isotope analyses.— Prior to analyses, the subsamples were treated for 48 hours with H<sub>2</sub>O<sub>2</sub> (30%) to remove residual organic matter, rinsed three times with ultrapure water, and dried overnight in a vacuum oven at 30°C. Stable C – isotope analyses of carbonates were performed by immersing whole-rock powders in 100% phosphoric acid while under vacuum (McCrea, 1950) and analyzing the released CO<sub>2</sub> on a Finnegan MAT 252 mass spectrometer. Since the samples investigated did not permit a physical separation of the dolomite from the minor amounts of calcite also present in the samples, a chemical separation technique was used which allowed CO<sub>2</sub> released from calcite and dolomite to be collected separately. This method is principally based on the marked difference in the relative rates of reaction between dolomite and calcite when treated with phosphoric acid. The carbon and oxygen isotopic data are

reported with respect to deviation from VPDB (Vienna Pee Dee Belemnite) using the standard  $\delta$  – notation (Craig, 1957; Craig, 1961)

Sr isotope analyses.— The small dolomite crystal size (average  $\sim 80~\mu m$ ) precluded micro sampling of specific zones within crystals, and thus grounded bulk samples were used for isotope analyses. The powder samples were digested by using a dilute acid (6N HCl). During the measuring period, the NIST 987 standard yielded 0.710250 and the internal precision ('error') associated with the strontium isotopic analysis was from 0.000016 to 0.000018 ( $2\sigma$  level). The radiogenic Sr isotope analyses were performed by Robert A. Creaser at the University of Alberta.

To provide an estimate of the initial Sr isotope signature of the carbonate fraction, we first evaluate to what extent the bulk Sr isotope composition of these rocks correlates with indicators of detrital contamination. This was accomplished by assessing the correlation between the <sup>87</sup>Sr/ <sup>86</sup>Sr signature of the samples and K, Zr, and rare earth elements (REEs) (Kamber and others, 2004). This test of isotopic integrity allowed us to establish the degree of correlation between the <sup>87</sup>Sr/ <sup>86</sup>Sr isotope ratios and such trace elements, with a high level of correlation indicating that the isotope (and trace element) systems remained closed during burial (see Kamber and others, 2004 for details). Then the isotope value of an uncontaminated sample can be inferred (see Kamber and others, 2004 for details).

# In Situ Analyses

For the detection and spatial substantiation of subtle crystal – scale chemical differences in dolomite crystals, we used a combination of LA-ICPQ-MS and high – resolution photon microprobe analyses (see below). Analyses were performed using a Perkin-Elmer Elan6000 Quadrupole ICPQ – MS coupled to a New Wave UP – 213 laser ablation system. The instrument parameters were as follows: RF power 1200 W, peak hopping acquisition, 50 ms dwell time. The crystals were ablated (60  $\mu$ m spot, 15 Hz) in a discrete spot mode at laser fluence on target of ~4 J/cm². Ablation took place in a He atmosphere (850 ml/min continuous He flow) to which both Ar (~450 ml/min) and N₂ (6 ml/min) were added downstream of the LA cell. Quantitative results were obtained via calibration of relative element sensitivities against the pressed powder carbonate standard pellet USGS MACS-3, with [Ca] determined via EPMA as an internal standard. Although the complete range of elemental masses certified in the MACS-3 standard

were measured, here we focus predominately on results for V, Ni, Fe, Mn, Zn, Sr, REE and Y. Quantitative elemental analysis provides relative accuracy of better than 8%

The distribution of trace elements in dolomite crystals was assessed via spatially resolved synchrotron-based X ray Fluorescence ( $\mu$ XRF). These analyses were conducted in the photon microprobe of the beamline 20ID at the Advanced Photon Source, Argonne National Laboratories (APS) in Argonne, IL. The analytical capabilities of this beamline not only allowed for an assessment of subtle micrometer-scale variations in the distribution of the first row transition metals, but also semi – quantitative analyses of their concentrations over a reduced analytical area; a highly desired feature when studying the geochemistry of fine dolomite crystals. X rays tuned at 20.96 KeV were focused to a 5 × 6-micron spot using Kirkpatrick-Baez mirrors and rastered across an analytical area of a representative sample (UD – 171 16 245.8°). The resulting fluorescence spectra were measured using a 4 – element Vortex multi – element Si drift detector located at 90° to the incident beam in the direction of the polarization. The detector was calibrated to ~30 eV per channel. Element – specific maps were then made to show hot spots of accumulation (for instance Sr, Y, and Mn enriched zones). A homogenous area at the microscale on the USGS' MACS-3 was used as an external standard.

## Correlation of Discrete Parameters

A Spearman rank correlation coefficient (R<sub>s</sub>) was used as a non-parametric measure of the strength and direction of association between any two parameters of interest. Possible correlations between multiple biogeochemical parameters were assessed by applying a Principal Component Analyses of scored data using XLStat 2014.

#### REFERENCES FOR ANALYTICAL METHODS

- Brocks, J., and Summons, R., 2003, Sedimentary hydrocarbons, biomarkers for early life. Treatise on Geochemistry v. 8, p. 63–115.
- Brocks, J. J., Love, G. D., Summons, R. E., Knoll, A. H., Logan, G. A., and Bowden, S. A., 2005. Biomarker evidence for green and purple sulphur bacteria in a stratified Paleoproterozoic sea. Nature, v. 437, p. 866–870
- Brocks, J. J., and Hope, J. M., 2014, Tailing of chromatographic peaks in GC–MS caused by interaction of halogenated solvents with the ion source: Journal of Chromatographic Science, v. 52, p. 471–475.
- Canfield, D. E., Raiswell, R., Bottrell, S., 1992, The reactivity of sedimentary iron minerals toward sulfide: American Journal of Science, v. 292, p. 659–683.

- Craig, H., 1957, Isotopic standards for carbon and oxygen and correction factors for mass–spectrometric analysis of carbon dioxide: Geochimica et Cosmochimica Acta, v. 12, p. 133–149.
- Craig, H., 1961, Standards for reporting concentrations of deuterium and oxygen–18 in natural waters: Science, v. 133, p. 1833–1834.
- de Baar, H., German, C., Elderfield, H., van Gaans, P., 1988. Rare earth element distributions in anoxic waters of the Cariaco Trench: Geochimica et Cosmochimica Acta, v. 52, p. 1203–1219.
- de Baar, H. J. W., Schijf, J., and Byrne, R. H., 1991, Solution chemistry of the rare earth elements in seawater: Solid State Inorganic Chemistry, v. 28, p. 357–373.
- Jones, B., Luth, R. W., MacNeil, A. J., 2001, Powder X ray diffraction analysis of homogeneous and heterogeneous sedimentary dolostones: Journal of Sedimentary Research, v. 71, p. 790–799.
- Kamber, B. S., Bolhar, R., Webb, G. E., 2004, Geochemistry of late Archaean stromatolites from Zimbabwe: evidence for microbial life in restricted epicontinental seas: Precambrian Research v. 132, p. 379–399.
- McCrea, J.M., 1950, On the isotopic chemistry of carbonates and a paleotemperature scale: The Journal of Chemical Physics, v. 18, p. 849–857
- Nance, W. B., Taylor, S. R., 1976, Rare earth patterns and crustal evolution: I. Australian post-Archean sedimentary rocks: Geochimica et Cosmochimica Acta, v. 40, p. 1539–155.
- Poulton, S. W., Raiswell, R., 2002. The low–temperature geochemical cycle of iron: from continental fluxes to marine sediment deposition: American Journal of Science, v. 302, p. 774–805.
- Poulton, S. E, Canfield, D. E., 2005, Development of a sequential extraction procedure for iron: implications for iron partitioning in continentally derived particulates: Chemical Geology, v. 214, p. 209–221.
- Poulton, S. W., Canfield, D. E., 2011, Ferruginous Conditions: A Dominant Feature of the Ocean through Earth's History: Elements, v. 7, p. 107–112.
- Raiswell, R., Canfield, D. E., 1998, Sources of iron for pyrite formation in marine sediments: American Journal of Science, v. 298, p. 219–245.
- Shen, Y. N., Canfield, D. E., Knoll, A. H., 2002. Middle Proterozoic ocean chemistry: evidence from the McArthur Basin, northern Australia: American Journal of Science, v 302, p. 81–109
- Staudt, W., Oswald, E., Schoonen, M., 1993, Determination of sodium, chloride and sulfate in dolomites: a new technique to constrain the composition of dolomitizing fluids: Chemical Geology v. 107, p. 97–109.
- Wedepohl, K. H., 1978, Manganese: abundance in common sediments and sedimentary rocks, *in* Wedepohl, K. H., editor, Handbook of Geochemistry, Berlin, Springer, p. 1–17.

#### DETAILS ON BIOMARKERS

#### n-alkanes

n-Alkanes in most samples range from n-C<sub>12</sub> to n-C<sub>38</sub> and have unimodal (samples 3, 4, 5, 6, 8, 9, 10), bimodal (1, 2) or trimodal (7) distribution patterns (fig. SI.1; for sample numbers see table 1). In samples 2, 5, 6, 7 and 8, a dominance of n-alkanes with odd carbon numbers in the range C<sub>26</sub> to C<sub>34</sub> (CPI<sub>26-34</sub> = 1.1 – 1.3) implies that a proportion of organic matter was derived from waxes of terrestrial vascular plants (Eglinton and others, 1962; Dembicki and others, 1976). An odd-over-even carbon number preference for n-alkanes in the range C<sub>15</sub> to C<sub>23</sub> (EOP<sub>15-23</sub> < 1.0), which is suggestive of algal or cyanobacterial organic matter input (for example Gelpi and others, 1970), is only observed in a single sample. More common is an even carbon number preference (table 1) that may be caused by the reduction of fatty acids in reducing environments or direct microbial input (Grimalt and Albaigés, 1987).

# Acyclic isoprenoid

Most samples contain regular (head-to-tail linked) acyclic isoprenoids (i- $C_x$ ) with 16 to 25 carbon atoms (for example fig. SI.2). Pseudohomologues with  $\ge C_{21}$  carbon atoms are probably largely derived from archaea (Illich, 1983; Volkman, 1986), while pseudohomologues with  $C_{16}$  to  $C_{20}$  carbon atoms are predominantly regarded as degradation products of the phytol side chain of (bacterio)chlorophylls of phototrophic organisms. The acyclic isoprenoids pristane (Pr, i- $C_{19}$ ) and phytane (Ph, i- $C_{20}$ ) are oxidation and reduction products of the phytol side chain of chlorophyll, respectively (Powell and McKirdy, 1973). Thus, the ratio of pristane to phytane (Pr/Ph) is a useful parameter to assess redox conditions in the depositional environment (Didyk and others, 1978). The Pr/Ph in the Maracaibo shales studied fall into a very broad range (Pr/Ph = 0.29 to 3.4, table 1). Peters and others (2005) suggests that high Pr/Ph ratios (> 3.0) indicate influx of terrigenous, soil-derived and oxidized organic matter, while low values (< 0.8) point to anoxic aqueous environments. Thus, organic matter in the Maracaibo samples appears to be of mixed terrestrial and marine origin.

Other tentatively identified isoprenoids have irregular head-to-head ( $C_{32}$  to  $C_{40}$ ) and tail-to-tail ( $C_{20}$ , crocetane;  $C_{25}$ , 2,6,10,15,19-pentamethylicosane, PMI;  $C_{30}$ , squalane) branched structures, which are probably largely derived from archaea (Moldowan and Seifert, 1979;

Rowland, 1990). However, crocetane can also be a degradation product of aromatic carotenoids, and squalane precursors occur in organisms from all three domains of life (Maslen and others, 2009 and references therein).

# Polycyclic terpanes

Similar to other reports for the mid-Cretaceous (Dumitrescu and Brassell, 2005 and references therein), our samples contained  $13\beta(H)$ , $14\alpha(H)$ -tricyclic terpanes in the range  $C_{19}$  to  $C_{26}$  (maximum at  $C_{23}$ ) and a complete homologue series of  $17\alpha(H)$ , $21\beta(H)$ -homopanes with 27 to 35 carbon atoms (maximum at  $C_{30}$  or  $C_{31}$ ). Minor components are  $C_{29}$  to  $C_{31}$   $\beta\alpha$ -hopanes (moretanes), 28,30-bisnorhopanes and  $C_{29}$  to  $C_{31}$  diahopanes. Oleanane and bicadinane were also detected in trace amounts. These  $C_{30}$  pentacyclic terpanes are diagnostic for higher terrestrial plants (Moldowan and others, 1984; Zumberge, 1987.), but their abundance in the dolomitic shales is lower than reported in previous studies of the Maracaibo Platform (Alberdi – Genolet and López, 2000).

Gammacerane ( $\gamma$ ) is also present in all samples (for example fig. SI.3). This pentacyclic terpane is formed in sediments by defunctionalization of tetrahymanol (gammaceran-3 $\beta$ -ol) (Ten Haven and others, 1989; Sinninghe-Damsté and others, 1995). Tetrahymanol is found in nitrogen-fixing bacteria, purple non-sulfur bacteria, rumen fungus, fern and in heterotrophic marine as well as lacustrine ciliates, and occurs ubiquitously in marine sediments (Venkatesan, 1989). In stratified marine environments, anaerobic ciliates are probably the most significant source of tetrahymanol (Sinninghe-Damsté and others, 1995). These organisms thrive at or beneath the chemocline in dense populations, causing elevated values of the gammacerane index (GI =  $\gamma$  / ( $\gamma$  + C<sub>30</sub>  $\alpha\beta$ -hopane)). In the dolomitic shales from the Maracaibo ramp, values range from 1.1 to 18% (table 1). Although cut-off values do not exist, elevated GI ratios (> 5%) are commonly interpreted as indicators of water column stratification, which may be associated with bottom water hypersalinity and reducing conditions (Ten Haven and others, 1988; Harvey and Mcmanus, 1991; Sinninghe-Damsté and others, 1995).

A high gammacerane index (GI), a measure of the abundance of ciliates, is common in stable stratified aquatic ecosystems (Sinninghe-Damsté and others, 1995). In the Maracaibo samples, GI is lowered during periods of maximal terrestrial run-off. This observation is

counterintuitive as the influx of freshwater should intensify the density difference between deep and shallow waters and lead to rising GI values (for instance Erbacher and others, 2001).

Decreasing GI values despite enhanced freshwater influx may have two explanations. Firstly, a decline in gammacerane production may be related to famine of ciliate populations. Ciliates commonly feed on anoxygenic phototrophs and other dense populations of bacteria that inhabit the chemocline within the photic zone. However, elevated terrestrial run-off probably caused turbid conditions. Towards the outer to middle ramp setting, it is plausible that the shading effect of suspended particles reduced the depth of the photic zone so that the base did not reach into anoxic bottom waters. This would have caused diminishing populations of anoxygenic phototrophs, thus affecting ciliate communities (fig. 9). Secondly, GI values may be depressed during influx of terrestrial organic matter by a dilution effect. GI is defined as the ratio of gammacerane over C<sub>30</sub> hopane. Thus, simple influx of hopanoid-rich soil material may have contributed to declining GI values. However, the very wide range of GI (1.1 to 18.2 %) suggests that ecological effects must have played a role as well.

A complete series of  $2\alpha$ - and  $3\beta$ - $C_{31}$  to  $C_{36}$  A-ring methylated hopanes is present, with  $C_{32}$  as the most dominant homologue.  $2\alpha$ - and  $3\beta$ -methylhopane indices (2MHI and 3MHI) measure the abundance of  $C_{31}$  methylhopanes relative to the corresponding  $C_{30}$   $\alpha\beta$ -hopane (MHI =  $C_{31}$  methylhopane / ( $C_{31}$  methylhopane +  $C_{30}$   $\alpha\beta$ -hopane)). For the Maracaibo samples, 2MHI = 2.3 to 6.6% and 3MHI = 1.5 to 7.3% (table 1). The precursor molecule of  $2\alpha$ -methylhopanes, 2-methylbacteriohopanetetrol, was initially proposed to be exclusively produced by photosynthesizing cyanobacteria (Summons and others, 1999). However, recent work argues that sedimentary 2-methylhopanes are more typically associated with environmental niches with low oxygen levels, and a dominance of nitrogen-fixing organisms thriving within a sessile microbial community, such as microbial mats and stromatolites (Ricci and others, 2013). Precursors of  $3\beta$ -methylhopanes are known from microaerophilic methanotrophs (Neunlist and Rohmer, 1985) and acetobacteria (Simonin and others, 1994).

Another compound class detected in the mid-Cretaceous shales are  $C_{30}$  tetracyclic polyprenoids (TPP), which are believed to derive from freshwater algae. The ratio of these molecules with 27-nor(dia)cholestanes varies between 0.48 and 0.83. Values in this range are

interpreted as influx of organic matter from freshwater environments into a marine depositional system (Holba and others, 2003).

#### Steranes

Steranes and aromatic steroids are abundant in all samples and comprise most of the known  $C_{26}$  to  $C_{30}$  pseudohomologues, diasteranes, A-ring methylated steranes, and mono- and tri-aromatic steroids (for example fig. SI.3). The ratio between eukaryotic steranes and bacterial hopanes (Ster/Hop) fluctuates widely between 0.13 and 1.1 (table 1). Both cholestane ( $C_{27}$ ) and stigmastane ( $C_{29}$ ) fluctuate widely within a similar range (32 to 45% and 29 to 44%, respectively), whereas ergostane ( $C_{28}$ ) constitutes about 25% in all but one sample. Variations in Mesozoic stigmastane ( $C_{29}$ ) abundances are commonly explained by changing organic matter input from terrestrial plants (Grantham and Wakefield, 1988). 24-n-propylcholestane, a  $C_{30}$  sterane, is a diagnostic marine indicator since the precursor sterols are produced by marine foraminifera or marine benthic microalgae of the order Sarcinochrysidales (Huang and Meinschein, 1979; Raederstorff and Rohmer, 1984; Volkman, 2003; Grabenstatter and others, 2013). In the Maracaibo, the abundance of this  $C_{30}$  sterane relative to the sum of  $C_{27}$  to  $C_{30}$  steranes varies between 1 and 4% (table 1); again implying varying marine organic matter contributions.

#### Carotenoid derivatives

We have identified in the saturated hydrocarbon fraction intact  $C_{40}$  carotenoid derivatives lycopene,  $\beta$ -carotane and  $\gamma$ -carotane using relative retention time and mass spectra. Fig. SI.4 shows the corresponding signals in traces of the characteristic molecular ion. The m/z = 125 trace reveals further unidentified compounds that may represent isomers of  $\gamma$ - and  $\beta$ -carotane. Lycopane does co-elute most likely with a  $C_{40}$  isoprenoid, and  $\gamma$ -carotane is co-eluting with  $C_{36}$  n-alkane.

Saturated and aromatic carotenoid derivatives are discussed in Appendix B of the main text.

## Other aromatic compounds

 $C_{32} - C_{35}$  Benzohopanes and to a lesser extent  $C_{31} - C_{34}$  aromatic secohopanoids are also detected in the aromatic fraction of most of the samples. Dibenzothiophene are also present and their concentrations vary from <1 to 33 ppm.

#### REFERENCES FOR DETAILS ON BIOMARKERS

- Alberdi-Genolet, M. and Tocco, R., 1999, Trace metals and organic geochemistry of the Machiques Member (Aptian Albian) and La Luna Formation (Cenomanian Campanian), Venezuela: Chemical Geology, v. 160, p. 19–38.
- Alberdi-Genolet, M. and López, L., 2000, Biomarker 18α (H)-oleanane: a geochemical tool to assess Venezuelan petroleum systems: Journal of South American Earth Sciences, v. 13, p, 751–759.
- Bray, E. and Evans, E., 1961, Distribution of *i*-paraffins as a clue to recognition of source beds: Geochimica et Cosmochimica Acta v. 22, p, 2–15.
- Brocks, J. J. and Hope, J. M., 2014, Tailing of chromatographic peaks in GC-MS caused by interaction of halogenated solvents with the ion source: Journal of Chromatographic Science, v. 52, p. 471–475.
- Brocks, J. J., Love, G. D., Summons, R. E., Knoll, A. H., Logan, G. A., and Bowden, S. A., 2005, Biomarker evidence for green and purple sulphur bacteria in a stratified Palaeoproterozoic sea: Nature v. 437, p. 866–870.
- Brocks, J. J. and Schaeffer, P., 2008, Okenane, a biomarker for purple sulfur bacteria (Chromatiaceae), and other new carotenoid derivatives from the 1640Ma Barney Creek Formation: Geochimica et Cosmochimica Acta, v. 72, p. 1396–1414.
- Brocks J. J. and Summons R. E., 2004, Sedimentary hydrocarbons, biomarkers for early life, in D. Holland and K. K. Turekian, Treatise on Geochemistry: Amsterdam, Elsevier, v. 8, p. 63–115.
- Brooks, J., Gould, K., and Smith, J., 1969, Isoprenoid hydrocarbons in coal and petroleum: Nature v. 222, p. 257–259.
- Cao, C., Love, G. D., Hays, L. E., Wang, W., Shen, S., and Summons, R. E., 2009, Biogeochemical evidence for euxinic oceans and ecological disturbance presaging the end–Permian mass extinction event: Earth and Planetary Science Letters, v. 281, p. 188–201.
- Dembicki Jr., H., Meinschein, W. G., and Hattin, D. E., 1976, Possible ecological and environmental significance of the predominance of even-carbon number  $C_{20} C_{30}$  n-alkanes: Geochimica et Cosmochimica Acta, v. 40, p. 203–208.
- Dumitrescu, M. and Brassell, S. C., 2005, Biogeochemical assessment of sources of organic matter and paleoproductivity during the early Aptian Oceanic Anoxic Event at Shatsky Rise, ODP Leg 198: Organic Geochemistry, v. 36, p. 1002–1022.

- Eglinton, G., Gonzalez, A. G., Hamilton, R. J., and Raphael, R. A., 1962, Hydrocarbon constituents of the wax coatings of plant leaves: A taxonomic survey: Phytochemistry, v. 1, p. 89–102.
- Erbacher, J., Huber, B. T., Norris, R. D., and Markey, M., 2001, Increased thermohaline stratification as a possible cause for an ocean anoxic event in the Cretaceous period: Nature, v. 409, p. 325–327.
- Gelpi, E., Schneider, H., Mann, J., and Oro, J., 1970, Hydrocarbons of geochemical significance in microscopic algae: Phytochemistry, v. 9, p. 603–612.
- Grabenstatter, J., Méhay, S., McIntyre-Wressnig, A., Giner, J. L., Edgcomb, V. P., Beaudoin, D. J., Bernhard, J. M., and Summons, R. E., 2013. Identification of 24-n-propylidenecholesterol in a member of the Foraminifera: Organic Geochemistry, v. 63, p. 145–151.
- Grantham, P. J. and Wakefield, L. L., 1988, Variations in the sterane carbon number distributions of marine source rock derived crude oils through geological time: Organic Geochemistry, v. 12, p. 61–73.
- Grimalt, J. and Albaigés, J., 1987, Sources and occurrence of C<sub>12</sub> C<sub>22</sub> n-alkane distributions with even carbon number preference in sedimentary environments: Geochimica et Cosmochimica Acta, v. 51, p. 1379–1384.
- Harvey, H. R. and Mcmanus, G. B., 1991, Marine ciliates as a widespread source of tetrahymanol and hopan-3β-ol in sediments: Geochimica et Cosmochimica Acta, v. 55, p. 3387–3390.
- Holba, A., Dzou, L., Wood, G., Ellis, L., Adam, P., Schaeffer, P., Albrecht, P., Greene, T., and Hughes, W., 2003, Application of tetracyclic polyprenoids as indicators of input from freshbrackish water environments: Organic Geochemistry, v. 34, p. 441–469.
- Huang, W. -Y. and Meinschein, W. G., 1979, Sterols as ecological indicators: Geochimica et Cosmochimica Acta, v. 43, p. 739–745.
- Illich, H. A., 1983, Pristane, phytane, and lower molecular weight isoprenoid distributions in oils: American Association of Petroleum Geologists Bulletin, v. 67, p. 385–393.
- Krügel, H., Krubasik, P., Weber, K., Saluz, H. P., and Sandmann, G., 1999, Functional analysis of genes from Streptomyces griseus involved in the synthesis of isorenieratene, a carotenoid with aromatic end groups, revealed a novel type of carotenoid desaturase. Biochimica et Biophysica Acta (BBA) Molecular and Cell Biology of Lipids 1439, 57–64.
- Mallory, F. B., Gordon, J. T., and Conner, R. L., 1963. The isolation of a pentacyclic triterpenoid alcohol from a protozoan: Journal of the American Chemical Society 85, 1362–1363.
- Maslen, E., Grice, K., Gale, J. D., Hallmann, C., and Horsfield, B., 2009, Crocetane: a potential marker of photic zone euxinia in thermally mature sediments and crude oils of Devonian age: Organic Geochemistry, v. 40, p. 1–11.
- Moldowan, J. M. and Seifert, W. K., 1979, Head-to-head linked isoprenoid hydrocarbons in petroleum: Science v. 204, p. 169–171.

- Moldowan, J. M., Seifert, W. K., and Gallegos, E. J., 1985, Relationship between petroleum composition and depositional environment of petroleum source rocks: American Association of Petroleum Geologists Bulletin, v. 69, p. 1255–1268.
- Neunlist, S. and Rohmer, M., 1985, Novel hopanoids from the methylotrophic bacteria *Methylococcus capsulatus* and *Methylomonas methanica* (22S)-35-aminobacteriohopane-30,31,32,33,34-pentol and (22S)-35-amino-3 beta-methylbacteriohopane-30,31,32,33, 34-pentol: Biochemical Journal, v. 231, p. 635–639.
- Peters, K. E., Walters, C. C., and Moldowan, J. M., 2005, The biomarker guide: Biomarkers and Isotopes in Petroleum Exploration and Earth History: Cambridge, Cambridge University Press.
- Powell, T. and McKirdy, D., 1973, Relationship between ratio of pristane to phytane, crude oil composition and geological environment in Australia: Nature v. 243, p. 37–39.
- Raederstorff, D. and Rohmer, M., 1984, Sterols of the unicellular algae *Nematochrysopsis roscoffensis* and *Chrysotila lamellosa*: isolation of (24E)-24-n-propylidenecholesterol and 24-n-propylcholesterol: Phytochemistry v. 23, p. 2835–2838.
- Ricci, J. N., Coleman, M. L., Welander, P. V., Sessions, A. L., Summons, R. E., Spear, J. R., and Newman, D. K., 2013, Diverse capacity for 2–methylhopanoid production correlates with a specific ecological niche: The ISME journal, v. 8, p. 675–684.
- Rowland, S., 1990, Production of acyclic isoprenoid hydrocarbons by laboratory maturation of methanogenic bacteria: Organic Geochemistry v. 15, p. 9–16.
- Simonin, P., Tindall, B., and Rohmer, M., 1994, Structure elucidation and biosynthesis of 31–methylhopanoids from *Acetobacter europaeus*: European Journal of Biochemistry, v. 225, p, 765–771.
- Sinninghe-Damsté, J. S., Kenig, F., Koopmans, M. P., Köster, J., Schouten, S., Hayes, J., and de Leeuw, J. W., 1995. Evidence for gammacerane as an indicator of water column stratification. Geochimica et Cosmochimica Acta 59, 1895–1900.
- Stephens, N. P. and Carroll, A. R., 1999. Salinity stratification in the Permian Phosphoria sea; a proposed paleoceanographic model. Geology 27, 899–902.
- Summons, R. E., Jahnke, L. L., Hope, J. M., and Logan, G. A., 1999. 2-Methylhopanoids as biomarkers for cyanobacterial oxygenic photosynthesis: Nature, v. 400, p. 554–557.
- Ten Haven, H., De Leeuw, J., Sinninghe-Damsté J. S., Schenck, P., Palmer, S., and Zumberge, J., 1988, Application of biological markers in the recognition of palaeohypersaline environments. Geological Society of London Special Publications, v. 40, p. 123–130.
- Ten Haven, H., Rohmer, M., Rullkötter, J., and Bisseret, P., 1989, Tetrahymanol, the most likely precursor of gammacerane, occurs ubiquitously in marine sediments: Geochimica et Cosmochimica Acta, v. 53, p. 3073–3079.
- Venkatesan, M. I., 1989, Tetrahymanol: Its widespread occurrence and geochemical significance: Geochimica et Cosmochimica Acta, v. 53, p. 3095–3101.
- Volkman, J., 2003, Sterols in microorganisms. Applied Microbiology and Biotechnology, v. 60, p. 495–506.

- Volkman, J. K., 1986, A review of sterol markers for marine and terrigenous organic matter. Organic Geochemistry v. 9, p. 83–99.
- Zumberge, J. E., 1987, Prediction of source rock characteristics based on terpane biomarkers in crude oils: A multivariate statistical approach: Geochimica et Cosmochimica Acta v. 51, p. 1625–1637.

# **SUPPLEMENTARY FIGURES**

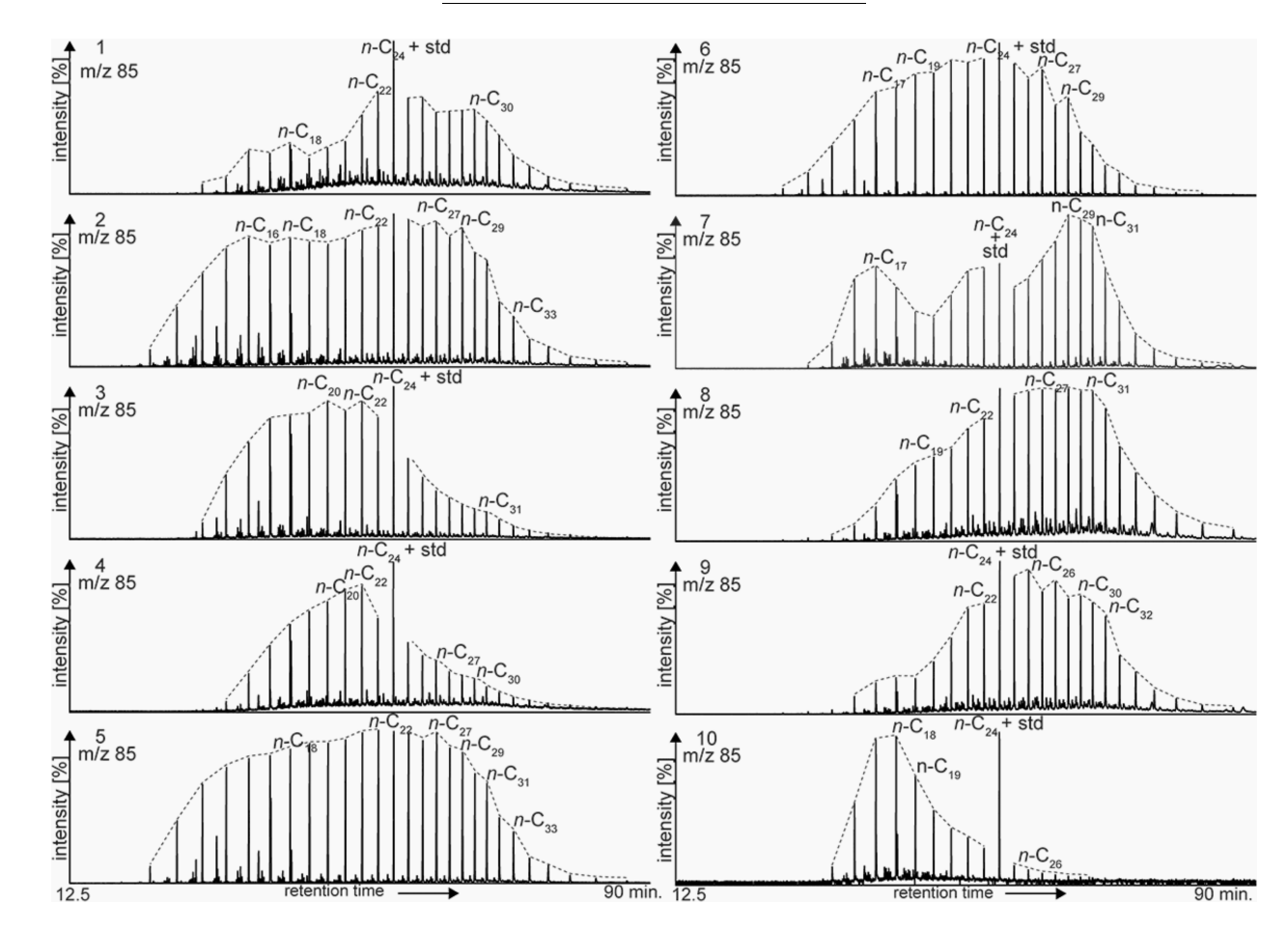


Fig. SI.1. Saturated hydrocarbons of all analyzed black shales: n-Alkane distributions vary between unimodal (2, 3, 4, 5, 6), bimodal (1, 8, 9), and trimodal (2, 3, 4, 5, 6) bimodal (1, 8, 9), and trimodal (2, 3, 4, 5, 6) bimodal (2, 3, 4, 5, 6), bimodal (2, 3, 4, 5, 6), and trimodal (2, 3, 4, 5, 6) bimodal (2, 3, 4, 5, 6), and trimodal (2, 3, 4, 5, 6) bimodal (2, 3, 4, 5, 6), bimodal (2, 3, 4, 5, 6), and trimodal (2, 3, 4, 5, 6) bimodal (2, 3, 4, 5, 6), and trimodal (2, 3, 4, 5, 6) bimodal (2, 3, 4, 5, 6), and trimodal (2, 3, 4, 5, 6) bimodal (2, 3, 4, 5, 6), and trimodal (2, 3, 4, 5, 6) bimodal (2, 3, 4, 5, 6), and trimodal (2, 3, 4, 5, 6) bimodal (2, 3, 4, 5, 6), and trimodal (2, 3, 4, 5, 6) bimodal (2, 3, 4, 5, 6), and trimodal (2, 3, 4, 5, 6) bimodal (2,

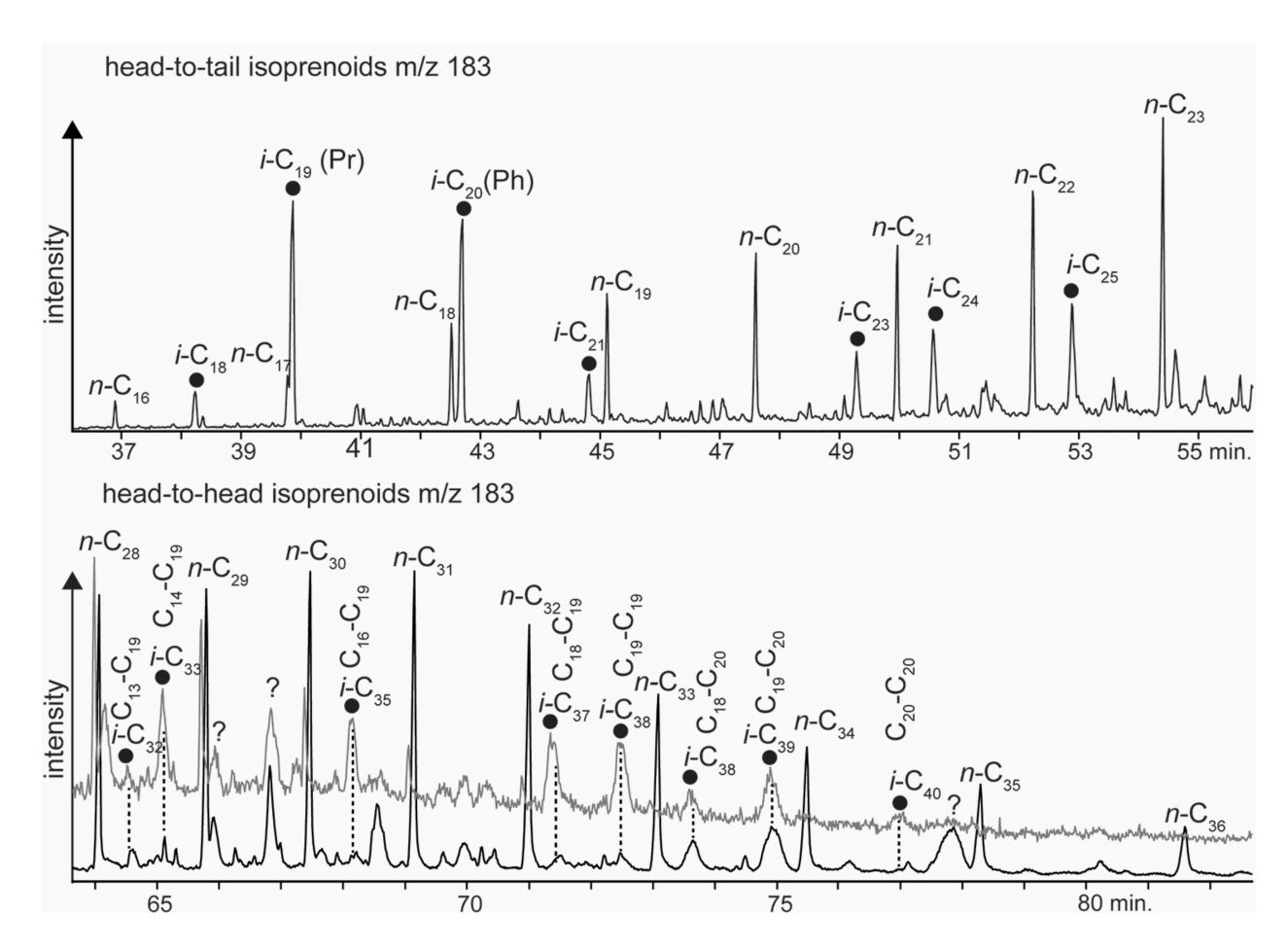


Fig. SI.2. Regular and irregular acyclic isoprenoids in saturated fractions of sample 8 from the Maracaibo ramp: (A) Head-to-tail isoprenoids (i- $C_x$ , x = carbon number) are shown in the m/z 183 trace. Black circles represent position of n-alkanes (n- $C_x$ , x = carbon number). (B) Irregular acyclic isoprenoid are identified by comparison with the reference (grcy) (Schinteie, 2011). Head-to-head homologue series of acyclic isoprenoids range from 32 to 40 carbon numbers (i- $C_x$ , x = carbon atoms).

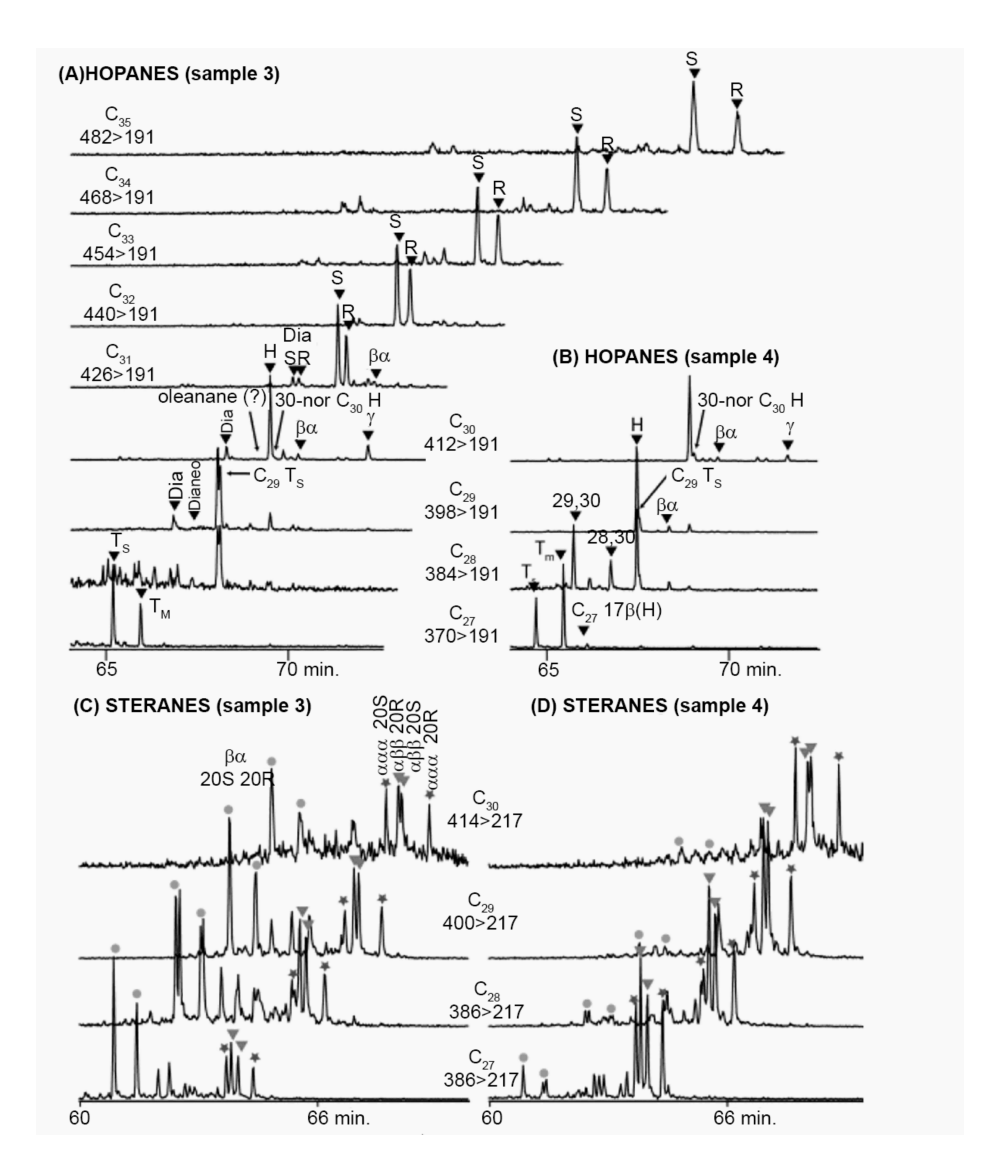


Fig. SI.3. MRM transitions showing terpanes and steranes of sample 3 and 4 (see table 1): (A) A complete homologue series of  $17\alpha(H)$ ,21 $\beta(H)$ -hopanes with 27 – 35 carbon atoms was detected in MRM M<sup>+</sup>  $\rightarrow$ 191 transitions, with the regular C<sub>30</sub>-hopane as the most abundant pentacyclic terpane. (B) Gammacerane ( $\gamma$ ) is clearly visible in the 412 > 191 transition. (C) Note that abundances can strongly vary, for example Tm, Ts and bisnorhopanes. (D) Steranes, detected in MRM M<sup>+</sup>  $\rightarrow$  217 transitions, comprise most of the known C<sub>26</sub> to C<sub>30</sub>-pseudohomologues and diasteranes. Abbreviations used: R and S are stereoisomers at C<sub>22</sub> or C<sub>20</sub> of the respective hopane or sterane,  $\beta\alpha = 17\beta(H)$ ,21 $\alpha(H)$ -hopanes = moretanes, Dia = diahopanes, Ts =  $18\alpha$ -22,29,30-trisnorneohopane, Tm =  $17\alpha$ -22,29,30-trisnorneohopane, 28,30 = 28,30-bisnorhopane, and 29,30 = 29,30-bisnorhopane. Circles represent diasteranes, triangles symbolize rearranged steranes, and stars localize normal steranes.

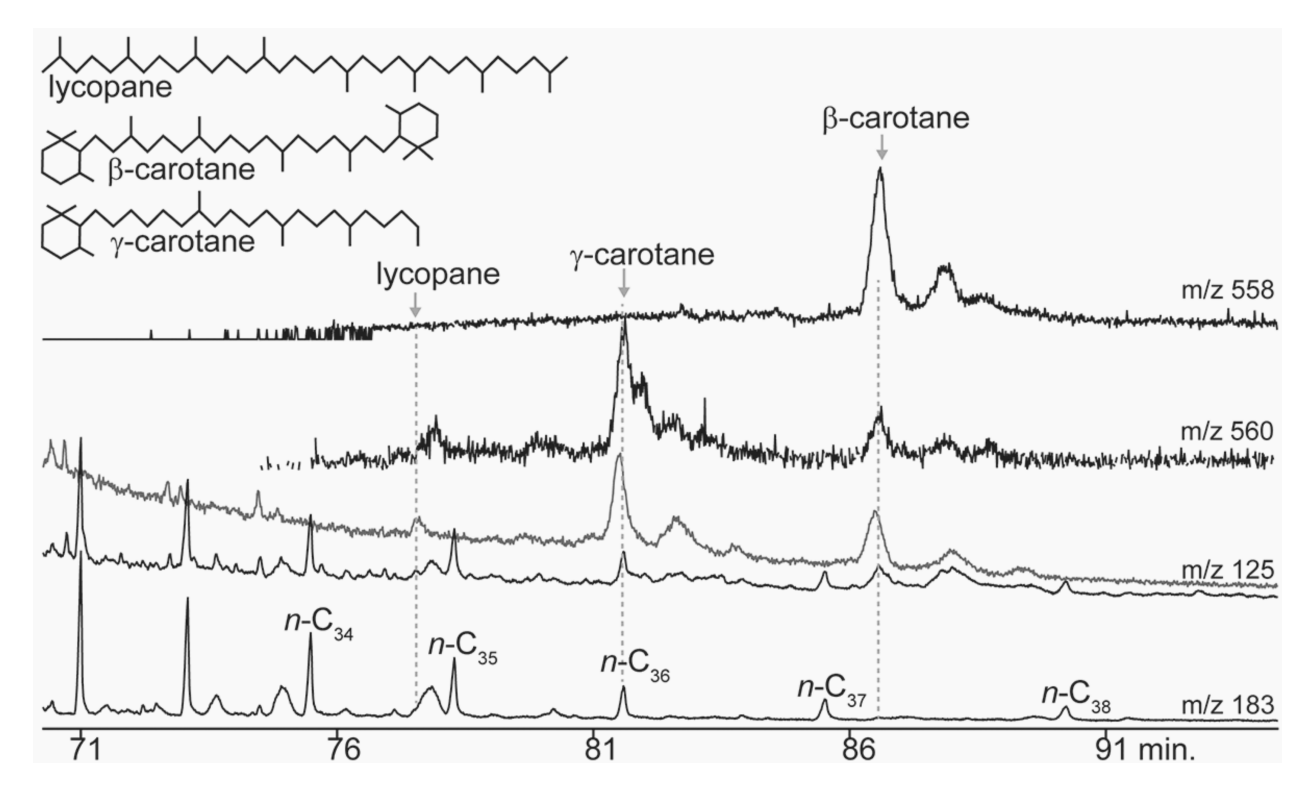


Fig. SI.4.  $C_{40}$  carotenoid derivatives in the saturated fraction of sample 8. Molecules are identified by comparison with a reference sample (gray) (Brocks and Schaeffer, 2008). Positions of *n*-alkanes and hopanes are indicated by n- $C_x$  and  $C_x$ H, respectively, with x =carbon atom number. Partial ion chromatograms of lycopane (m/z 125),  $\beta$ -carotane (m/z 561) and  $\gamma$ -carotane (m/z 559), the position of these molecules is shown.